PCCP

PAPER

View Article Online
View Journal | View Issue

Cite this: *Phys. Chem. Chem. Phys.*, 2017, **19**, 31216

High CO_2 absorption capacity by chemisorption at cations and anions in choline-based ionic liquids†

Shubhankar Bhattacharyya, *[a] Andrei Filippov *[ab] and Faiz Ullah Shah [a]

Received 17th October 2017,
Accepted 2nd November 2017

DOI: 10.1039/c7cp07059d

rsc.li/pccp

The effect of CO_2 absorption on the aromaticity and hydrogen bonding in ionic liquids is investigated. Five different ionic liquids with choline based cations and aprotic N-heterocyclic anions were synthesized. Purity and structures of the synthesized ionic liquids were characterized by ^1H and ^{13}C NMR spectroscopy. CO_2 capture performance was studied at 20 °C and 40 °C under three different pressures (1, 3, 6 bar). The IL $[N_{1,1,6,2OH}][4\text{-Triz}]$ showed the highest CO_2 capture capacity (28.6 wt%, 1.57 mol of CO_2 per mol of the IL, 6.48 mol of CO_2 per kg of the ionic liquid) at 20 °C and 1 bar. The high CO_2 capture capacity of the $[N_{1,1,6,2OH}][4\text{-Triz}]$ IL is due to the formation of carbonic acid ($-OCO_2H$) together with carbamate by participation of the –OH group of the $[N_{1,1,6,2OH}]^+$ cation in the CO_2 capture process. The structure of the adduct formed by CO_2 reaction with the IL $[N_{1,1,6,2OH}][4\text{-Triz}]$ was probed by using IR, ^{13}C NMR and ^1H–^{13}C HMBC NMR experiments utilizing ^{13}C labeled CO_2 gas. ^1H and ^{13}C PFG NMR studies were performed before and after CO_2 absorption to explore the effect of cation–anion structures on the microscopic ion dynamics in ILs. The ionic mobility was significantly increased after CO_2 reaction due to lowering of aromaticity in the case of ILs with aromatic N-heterocyclic anions.

Introduction

Ionic liquids (ILs) are typically low melting salts (usually <100 °C) comprising organic or inorganic cations and anions. Unique physicochemical properties such as high ionic conductivity, low vapor pressure, non-flammability and functional designability make ILs suitable sorbents for CO_2 as compared to the conventional molecular liquids. Though ILs have a wide range of properties, however, viscosity is always a major concern when they are used as CO_2 sorbents. Due to the presence of cations and anions in the same system, ILs are usually more viscous than other conventional molecular liquids.[1–3] Often ILs are regarded as designer solvents due to their tailor-made physicochemical properties by the manipulation of cation and anion structures. Extensive research efforts have already been made to understand and predict the macroscopic physicochemical properties of the ILs on the basis of their ionic interactions, microscopic ion dynamics, *etc.* Despite the extensive research efforts, the influence of cationic and anionic structures on the physicochemical properties of the ILs still remains a challenge. Thus, investigation of the ionic mobility of ILs is a promising area of research for the development of high performance ILs for challenging applications.[4,5]

Diffusivity (also known as self-diffusion) of molecules, ions and their aggregates is a property of any liquid as a result of thermal motion.[6] This property determines many of the physicochemical characteristics of a liquid such as viscosity, ionic conductivity, and adsorption, and also influences the mechanisms and rates of chemical reactions. In this regard, investigation of the diffusivity of ILs can help in gaining new insights and a better understanding of their ion dynamics, transport properties[7,8] and other technological processes.[7] Self-diffusion in ILs generally obeys the laws of diffusivity of molecules in liquids such as Gaussian statistics for mean-squared displacements and the Stokes–Einstein equation.[6] Moreover, self-association phenomena are quite typical for many ILs[9] that lead to a specific diffusivity of ions.[10–12,37] Absorption of gases is another type of association that also effects the diffusivity of ions.[13] Nuclear magnetic resonance (NMR) spectroscopy is an appropriate technique for the investigation of the diffusion of ions and sorbent additives in the ILs.[14]

Because of the prevalent industrial applications of ILs, they are also regarded as promising CO_2 sorbents. However, the higher viscosity of ILs compared to the conventional amine sorbents remains a challenge, limiting their applicability as CO_2 sorbents. Recently, great attention has been paid by researchers to develop less viscous IL CO_2 sorbents as a possible replacement for the conventional amine sorbents. The most promising ILs as CO_2 sorbents are amino acid based ionic liquids with phosphonium and ammonium cations.[15] One of the possible reasons is that amino acid based ILs have low

[a] *Chemistry of Interfaces, Luleå University of Technology, Luleå SE-97187, Sweden. E-mail: shubhankar.bhattacharyya@ltu.se, andrei.filipov@ltu.se*
[b] *Institute of Physics, Kazan Federal University, 420008 Kazan, Russia*

† Electronic supplementary information (ESI) available. See DOI: 10.1039/c7cp07059d

toxicity and faster reactivity towards CO_2 molecules. Recently we have reported that functionalized choline based amino acid ILs have excellent CO_2 capture capacity at room temperature and atmospheric pressure.[16] Additionally, the ILs with choline based cations are more attractive due to their low toxicity and biodegradability.[17–19] At the same time, ILs containing amino acid anions with simple choline cations are highly viscous due to hydrogen bonding. We have found that etherification of choline cations leads to a dramatically low viscosity.[16] Also by replacing amino acid anions with N-heterocyclic anions, the viscosity of the ILs decreased significantly with improved CO_2 capture capacity.[13] In addition, it was observed that most of the amino acid based ILs become highly viscous or solidified after CO_2 absorption. However, aprotic N-heterocyclic anion (AHA) based ILs remained liquid with much faster ionic mobility after reaction with CO_2 molecules. Detailed insights into the comparative physicochemical and CO_2 capture studies of amino acid and N-heterocyclic amine based ILs with a common cation $[N_{1,1,6,2OH}]^+$ are recently reported.[13]

CO_2 capture studies of some aprotic N-heterocyclic based anions with a phosphonium cation $[P_{6,6,6,14}]^+$ have already been reported by different research groups. For example, AHA based IL phosphonium cations were reported by Wang *et al.* who achieved a CO_2 capture capacity of up to 7.5 wt% (0.95 mol CO_2/IL) using $[P_{6,6,6,14}][4\text{-Triz}]$.[38] Then using the same phosphonium cation $[P_{6,6,6,14}]^+$, Brennecke's group reported on phosphonium indazolate $[P_{6,6,6,14}][\text{Inda}]$ based ILs with a maximum CO_2 absorption capacity of 7.1 wt% (0.98 mol CO_2/IL) under ambient pressure and temperature.[39] The regeneration of ILs often needs heating (up to 80 °C) with a continuous flow of nitrogen gas into the system. Furthermore, these CO_2 absorption capacities are significantly lower as compared to that of the traditional 2-aminoethanol (MEA or monoethanolamine) that has 29.9 wt% (0.42 mol) as a neat sorbent and 13.1 wt% capacity can also achieved by using 30% aqueous 2-aminoethanol (MEA) solution.[42] There is an urgent need to replace 2-aminoethanol with environmentally benign ILs having higher CO_2 capture capacity.

Apart from AHA based ILs, various protic ILs have also been reported for the CO_2 capture process. The major advantage of protic ILs is their low viscosity compared to AHA based ILs. However, CO_2 capture capacity and the process of regeneration of ILs have still not been improved. Zhu *et al.* recently reported on new 1,8-diazabicyclo[5.4.0]undec-7-ene (DBU) based protic ILs for CO_2 capture. However, the maximum CO_2 absorption capacity of DBU based protic ILs obtained for the IL $[DBUH^+][Im^-]$ was ~18 wt% (0.9 mol CO_2/IL).[40] Similarly, Dai *et al.* also reported 7-methyl-1,5,7-triazabicyclo[4.4.0]dec-5-ene (MTBD) superbase-derived protic IL $[MTBDH^+][Im^-]$ and showed a CO_2 absorption capacity of 17.0 wt% (1.03 mol CO_2 per mol of IL).[41] CO_2 capture by diamino based protic ILs has been reported by MacFarlane's group, although the maximum CO_2 uptake achieved was 12.6 wt% (0.47 mol CO_2 per mol of IL).[42] The CO_2 capture capacity of these ILs is not substantial (<20 wt%) compared to that of the traditional 2-aminoethanol (MEA) which also requires the energy demanding regeneration process to recycle the ILs. Therefore, there is a continuous quest for the development of new ionic liquids with high and reversible CO_2 absorption capacity with minimum energy input.

In this work, we investigate a comparison of the physiochemical properties as well as CO_2 capture capacities of different N-heterocyclic anion based ILs with functionalized choline as the cation. Five ILs having choline based cations and different aprotic N-heterocyclic anions were synthesized and characterized. The functionalized choline cation $[N_{1,1,6,2OH}]$ is further modified by etherification to study the effect of hydrogen bonding on the CO_2 absorption capacity, viscosity and ion mobility. FTIR, ^{1}H and ^{13}C NMR spectroscopic techniques were employed to characterize the structure of the adduct formed as a result of CO_2 reaction with the IL. In addition, ^{1}H NMR self-diffusion measurements were carried out on neat ionic liquids as well as after CO_2 absorption experiments using ^{1}H and ^{13}C pulsed field gradient (PFG) NMR techniques to understand the ionic mobility in these ILs. Density functional theory (DFT) calculations were performed to further support the experimental findings of the effect of CO_2 absorption on the ionic mobility of the ionic liquids.

Synthesis and characterization

All the reactants were purchased from Sigma Aldrich and used without further purification. Thin layer chromatographic analysis was carried out using silica gel 60 Å F-254 TLC plates with $KMnO_4$ charring solution.

All the ionic liquids were prepared using our previously reported procedures.[13] The excess of unreacted N-heterocycles was removed by adding excess of ACN and was stored over night at 0 °C. All the ILs were dried under vacuum at 60 °C for at least 2 days.

The ^{1}H and ^{13}C NMR characterization data for the synthesized ILs are given in the ESI.†

Water content was measured using a Metrohm 917 Karl Fischer Coloumeter with a HYDRANAL reagent. It was found that all ILs contain a water content of <0.5%.

Physicochemical characterization

The thermogravimetric analysis (TGA) of all the five ILs was performed using a Perkin Elmer 8000 TGA instrument in the temperature range from 30 °C to 550 °C with a heating ramp of 10 °C min^{-1} under a nitrogen atmosphere. 2–3 mg of the ionic liquid sample was used for each experiment. All the TGA experiments were performed under nitrogen gas as the inert carrier gas.

A Lovis 2000 ME Automated Microviscometer (Anton-Paar falling ball type viscometer with 2.50 mm glass capillary, viscosity range 10–10 000 cP) was used for viscosity measurement. The viscosity of the ILs was measured in the temperature range from 20 °C to 80 °C with a step size of 5 °C using a sealed glass capillary sample tube.

NMR and FTIR spectroscopy

A Bruker Ascend Aeon WB 400 (Bruker BioSpin AG, Fällanden, Switzerland) NMR spectrometer was used with a working

frequency of 400.22 MHz for ^{1}H and 100.65 MHz for ^{13}C. Bruker Topspin 3.5 software was used for the processing of data. All the spectra were recorded at 25 °C. Chemical shifts were expressed in parts per millions (δ) downfield from DSS with the solvent resonance as the internal standard (D_2O, δ = 4.79) and were reported as s (singlet), d (doublet), t (triplet), q (quartet), br (broad) and m (multiplet). All coupling constants (J) are reported in Hertz (Hz).

The ^{1}H and ^{13}C pulsed field gradient (PFG) NMR self-diffusion experiments were performed on a Bruker Ascend Aeon WB 400 instrument using a Diff50 (60 A) z-gradient 5 mm diffusion probe. A stimulated echo pulse sequence was employed,[14,20] with the diffusion coefficient (D) determined from the signal decay using the Stejskal and Tanner equation[20]

$$A(g) = A(0)\exp\left[-D\gamma^2 g^2 \delta^2 \left(\Delta - \frac{\delta}{3}\right)\right] \quad (1)$$

where $A(g)$ and $A(0)$ are the integral signal intensities obtained with and without gradient, respectively, γ is the gyromagnetic ratio for a used nucleus; g is the gradient strength, δ is the duration of the gradient pulse, $t_d = (\Delta - \delta/3)$ is the diffusion time, and Δ is the delay between the gradient pulses. A sample for the study was placed in a standard 5 mm glass sample tube and closed with a plastic stopper to avoid contact with air. Before each measurement, the sample was equilibrated at the specified temperature for 20 minutes. The experimental details of the PFG NMR technique can be found elsewhere.[14] Typical experimental conditions for ^{1}H PFG NMR included signal averaging with 16 scans, 32 gradient steps, a total gradient pulse length of δ = 1–2 ms, and a 5 s recycle delay. Δ was in the range from 30 to 200 ms. For the ^{13}C PFG NMR experiment the experimental conditions were: 3600 scans, 12 gradient steps, a total gradient length of δ = 0.1–2 ms, and a 5 s recycle delay. Δ was 10 ms.

Fourier transform infrared (FTIR) spectra were recorded on a Bruker IFS 80v vacuum Fourier transform infrared spectrometer equipped with a deuterated triglycine sulphate (DTGS) detector. All spectra were recorded at room temperature (~22 °C) using the double side forward–backward acquisition mode. A total number of 256 scans were co-added and signal-averaged at an optical resolution of 4 cm^{-1}.

CO_2 absorption measurement

CO_2 capture experiments were performed using ~0.1 g of neat ILs in a 10 ml Buchi stainless steel reactor with a PTFE insert and a pressure gauge. The CO_2 capture capacities of the ILs were measured at different pressures (1–6 bar) of CO_2 (99.999 by weight%) at 20 °C and 40 °C by weighing the PTFE insert gravimetrically using a Mettler Toledo analytical balance (0.1 mg accuracy).

Computational methods

DFT calculations were performed using GAUSSIAN 09[21] software packages. The B3LYP/6-311+g (d,p) level of theory was used for molecular geometry optimization. The optimized molecular geometries were characterized to be a relative energy minimum to the potential energy surface by real frequency. For NICS calculations the aug-cc-pvtz basis set was used. However, all calculations are performed under gas phase conditions, in the current calculations cations and the solvent model are not included as the solvent properties are not available for the IL structure.

Results and discussion

Five ILs with four different aprotic heterocyclic anions (imidazole, triazole, pyrazole, succinimide) were synthesized by following our previously reported procedures.[13] A choline based cation $[N_{1,1,6,2OH}]^+$ and a choline based ether functionalized cation $[N_{1,1,6,2O4}]^+$ are selected to investigate the effect of hydrogen bonding and ether functionalization on the ionic mobility before and after CO_2 absorption. To further investigate the effect of non-aromatic heterocyclic anions on the physico-chemical properties of ILs, the $[N_{1,1,6,2OH}][Succ]$ ionic liquid with a common cation $[N_{1,1,6,2OH}]^+$ and a succinimide anion was selected. Furthermore, the effect of ether functionalization on the cation was also studied using an ether functionalized ionic liquid $[N_{1,1,6,2O4}][4\text{-Triz}]$ in comparison with a non-ether functionalized ionic liquid $[N_{1,1,6,2OH}][4\text{-Triz}]$ having a common 1,2,4-triazolate anion $[4\text{-Triz}]^-$. The chemical structures and abbreviations of the ionic components of the studied ionic liquids are shown in Fig. 1.

Viscosity is one of the most influential physiochemical properties of ionic liquids used for various applications. Viscosity of the four different ionic liquids $[N_{1,1,6,2OH}][Im]$, $[N_{1,1,6,2OH}][4\text{-Triz}]$, $[N_{1,1,6,2OH}][Succ]$ and $[N_{1,1,6,2O4}][4\text{-Triz}]$, which were liquid at room temperature, was measured as a function of temperature (ESI,† S10). The ionic liquid $[N_{1,1,6,2O4}][Pyrz]$ was solid at room temperature. It was observed that viscosity of all these ILs is temperature dependent and can be fitted well into an Arrhenius form of equation for viscosity $\eta = \eta_0 \exp[E_a(\eta)/k_B T]$ for the measured temperature range from 20 °C to 80 °C, where η_0 and $E_a(\eta)$ are the constant and the activation energy for the viscous flow. From the Arrhenius equation for viscosity, the activation energy for the viscous flow was calculated. For less viscous ILs $[N_{1,1,6,2OH}][4\text{-Triz}]$ and $[N_{1,1,6,2OH}][Imi]$ the activation energies for viscous flow are 59.7 kJ mol^{-1} K^{-1} and 57.5 kJ mol^{-1} K^{-1}, respectively. It is interesting to note that the activation energy for viscous flow significantly decreased to 50.6 kJ mol^{-1} K^{-1} upon ether functionalization of the cation $[N_{1,1,6,2OH}]$. In addition, the activation energy for viscous flow increased significantly to 76.8 kJ mol^{-1} K^{-1} when an aromatic heterocyclic anion was replaced by a non-aromatic heterocyclic anion (succinimide anion).

It is observed that the IL with a non-aromatic heterocyclic anion (succinimide) was highly viscous at room temperature ($\gg$10 000 cP) compared to the other ionic liquids with aromatic anions. The viscosity of $[N_{1,1,6,2OH}][Succ]$ was measurable only at temperature higher than 50 °C using a falling ball viscometer. Although at 50 °C, the viscosity of $[N_{1,1,6,2OH}][Succ]$ was very high >9000 cP. However, as expected the viscosity of $[N_{1,1,6,2OH}][Succ]$ decreased significantly with the increase in

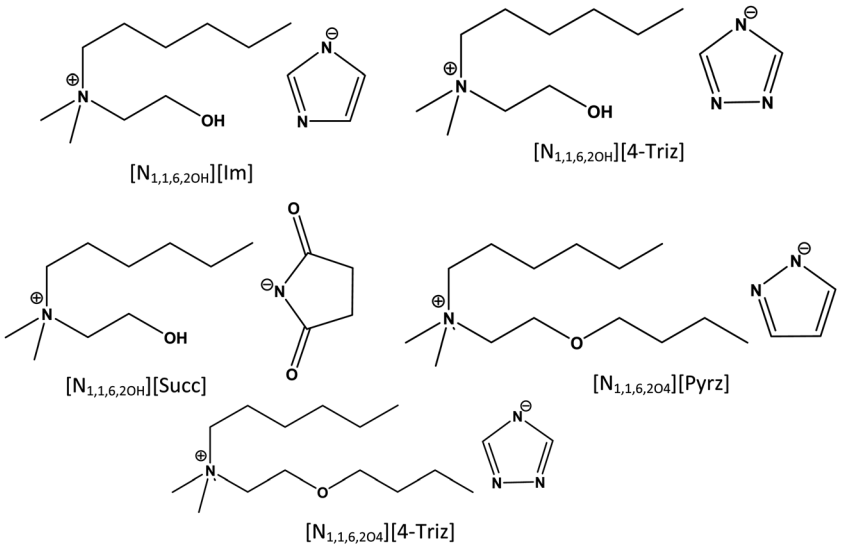

Fig. 1 Chemical structures and abbreviations of the ionic components of the choline based N-heterocyclic ionic liquids investigated.

temperature. At higher temperatures 80 °C, the viscosity dropped significantly to 803.7 cP (ESI,† S10).

Interestingly, the viscosity of ILs with aromatic heterocyclic anions was found to be significantly less as compared to ILs containing no N-heterocyclic anions with a common cation $[N_{1,1,6,2OH}]$. For example, at 20 °C the viscosities of $[N_{1,1,6,2OH}]$-[4-Triz] and $[N_{1,1,6,2OH}]$[Imi] were around 8953 cP and 4003 cP, respectively. With increasing temperature to 40 °C in the case of $[N_{1,1,6,2OH}]$[4-Triz], the viscosity decreased by 6 fold around 1570 cP, whereas for the IL $[N_{1,1,6,2OH}]$[Imi] the viscosity was less than 900 cP. Upon further increase in temperature to 60 °C, the viscosities of $[N_{1,1,6,2OH}]$[4-Triz] and $[N_{1,1,6,2OH}]$[Imi] decreased to 402.5 cP and 231 cP, respectively. At a higher temperature of 80 °C less difference in viscosity was observed for ILs $[N_{1,1,6,2OH}]$[4-Triz] and $[N_{1,1,6,2OH}]$[Imi]. The viscosity of the IL $[N_{1,1,6,2OH}]$[4-Triz] was always higher than that of the IL $[N_{1,1,6,2OH}]$[Imi] because the higher number of nitrogen atoms present in the triazole anion leads to stronger hydrogen bonding as compared to the imidazole anion.

To further investigate the effect of hydrogen bonding on the viscosity, we measured the viscosity of the ether functionalized IL $[N_{1,1,6,2O4}]$[4-Triz] in the same temperature range. From our previously reported work, we envision that etherification of choline based cations will lead to reduced H-bonding interactions resulting in less viscous ILs.[16] As expected, the viscosity of $[N_{1,1,6,2O4}]$[4-Triz] was found to be much lower, 1673 cP, at 20 °C as compared with $[N_{1,1,6,2OH}]$[4-Triz]. Further, upon increasing the temperature to 50 °C the viscosity further decreased to 204 cP, which is lower than the previously reported viscosity for the IL with the same anion and the $[P_{6,6,6,14}]^+$ cation.[22] It is probably due to a considerable hydrophobic interaction between the longer alkyl chains of the $[P_{6,6,6,14}]$[4-Triz] IL. At a high temperature of 80 °C the viscosity of $[N_{1,1,6,2O4}]$[4-Triz] was further lowered to 48 cP, whereas the viscosity of the IL $[P_{6,6,6,14}]$[4-Triz] was 69 cP. Although the viscosity of the IL decreased after ether functionalization, however, the IL $[N_{1,1,6,2O4}]$[4-Triz] became semi-solid after one day. In addition, we also studied the ether functionalized cation $[N_{1,1,6,2O4}]$ with a pyrazole anion. The IL $[N_{1,1,6,2O4}]$[Pyrz] was found to be a semi-solid at room temperature. This also indicates that hydrogen-bonding interactions play a key role in the solid–liquid behavior of ionic liquids. The viscosities of these choline-based ILs is still higher in comparison to those of protic ILs but most of the viscosity data are comparable with those of the previously reported AHA based ILs[38,39] by different groups. In addition these current viscosity studies can enrich our knowledge to design choline based low viscous AHA ILs for future applications.

Thermogravimetric analysis implies that upon ether functionalization of choline based cations the thermal stability of the ILs is decreased. Thermal degradation of the ether functionalized IL $[N_{1,1,6,2O4}]$[4-Triz] occurred around ~150 °C, whereas that of the non-ether functionalized IL $[N_{1,1,6,2OH}]$[4-Triz] occurred at ~160 °C. This also suggests that hydrogen-bonding interactions play a significant role in the thermal stability of ILs. However, the IL $[N_{1,1,6,2O4}]$[Pyrz] showed a relatively lower thermal stability (~120 °C). This is most probably due to the high reactivity of the nucleophilic pyrazole anion that decreases the thermal stability of this ionic liquid. The TGA curves are shown in the ESI† (S11).

The CO_2 capture performance of the five different ionic liquids was studied at 20 °C and 40 °C and three different pressures. The experiments were carried out gravimetrically with the neat ILs in closed pressure reactor with constant stirring. It is observed that the IL $[N_{1,1,6,2OH}]$[Succ] doesn't react with CO_2 even at elevated temperature (40 °C). This was confirmed by the absence of carbamate signal in the ^{13}C NMR spectrum for the IL $[N_{1,1,6,2OH}]$[Succ] after the CO_2 capture experiment. Most of the CO_2 was physically absorbed and the CO_2 solvation gradually increased with increasing pressure. At 20 °C under 6 bar pressure the CO_2 capture capacity of the IL $[N_{1,1,6,2OH}]$[Succ] was 2.1 wt% (0.13 mol of CO_2 per mol of the

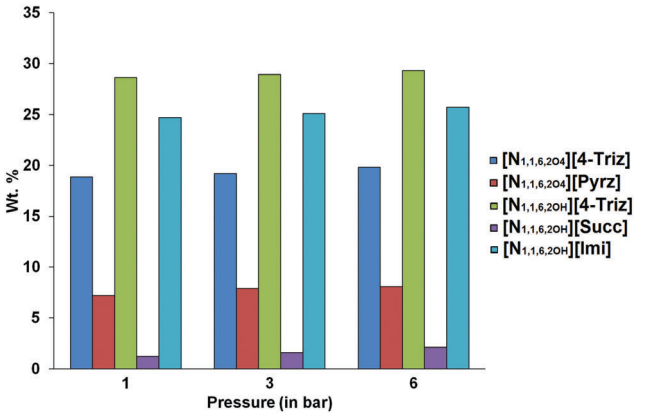

Fig. 2 CO_2 capture capacity of choline based N-heterocyclic ionic liquids at 20 °C.

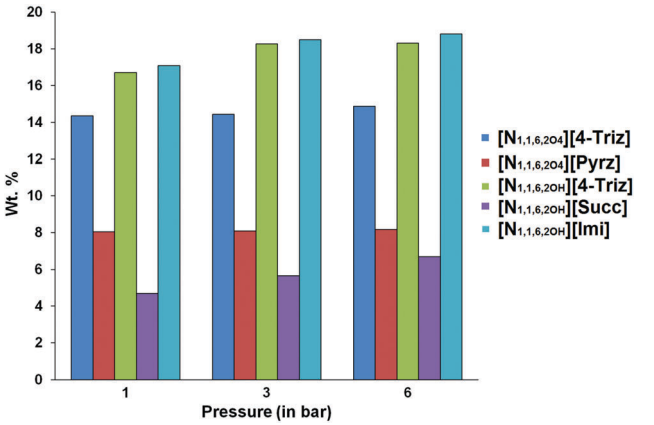

Fig. 3 CO_2 capture capacity of choline based N-heterocyclic ionic liquids at 40 °C.

IL). Surprisingly, at elevated temperature (40 °C) the CO_2 capture capacity of the IL $[N_{1,1,6,2OH}][Succ]$ increased by 3 fold (6.6 wt%, 0.4 mol of CO_2 per mol of IL at 6 bar). It is probably due to the decrease in viscosity at 40 °C, which leads to faster diffusion of CO_2 molecules in the IL (Fig. 2 and 3).

At 20 °C the IL $[N_{1,1,6,2OH}][4\text{-Triz}]$ showed the highest CO_2 capture capacity at lower (28.6 wt%, 1.57 mol of CO_2 per mol of IL at 1 bar) as well as higher pressure (29.3 wt%, 1.6 mol of CO_2 per mol of IL at 6 bar). Although the IL $[N_{1,1,6,2OH}][Imi]$ showed a slightly lower CO_2 capture capacity at 20 °C (24.7 wt%, 1.35 mol of CO_2 per mol of IL at 1 bar), however, the CO_2 capture capacity is increased to 25.7 wt% (1.4 mol of CO_2 per mol of IL) at higher pressure (6 bar). In order to further investigate the effect of ether functionalization of the $[N_{1,1,6,2OH}]^+$ cation, we performed the CO_2 capture experiment of the ether functionalized IL $[N_{1,1,6,2O4}][4\text{-Triz}]$. Surprisingly, after ether functionalization the CO_2 capture capacity decreased significantly. The CO_2 uptake capacity of the IL $[N_{1,1,6,2O4}][4\text{-Triz}]$ was 18.8 wt% (1.2 mol CO_2 per mol of IL) at 20 °C and 1 bar ambient pressure (Fig. 2). A slight increase in the CO_2 capture capacity was observed with the increase in pressure to 6 bar. The CO_2 uptake was 19.8 wt% (1.34 mol CO_2 per mol of IL) at 6 bar. The IL $[N_{1,1,6,2O4}][Pyrz]$, which is a semi-solid at room temperature, showed a lower CO_2 capture capacity (7.18 wt%, 0.48 mol of CO_2 per mol of IL) at 20 °C under 1 bar pressure compared to the aromatic N-heterocyclic anion based ILs. Even at higher pressure no such significant increase in the CO_2 capture capacity (8.09 wt%, 0.54 mol of CO_2 per mol of IL at 6 bar) was observed in the case of $[N_{1,1,6,2O4}][Pyrz]$.

The ILs $[N_{1,1,6,2OH}][4\text{-Triz}]$, $[N_{1,1,6,2O4}][4\text{-Triz}]$ and $[N_{1,1,6,2OH}][Imi]$ showed comparable capture capacity (~1 mol of CO_2 per mol of IL) at 40 °C. This revealed that chemisorption is predominant over other sorption phenomena at 40 °C (Fig. 3). The IL $[N_{1,1,6,2O4}][Pyrz]$ showed a relatively lower CO_2 capture capacity (~0.55 mol of CO_2 per mol of IL, ~8 wt% CO_2) at 40 °C, which is due to the less thermally stable carbamate anion formed after reaction with CO_2 molecules.

As the IL $[N_{1,1,6,2OH}][4\text{-Triz}]$ showed the highest CO_2 capture capacity at 20 °C compared to the other studied ILs, we further studied the recyclability of this particular IL. The desorption experiments were performed using a continuous stirring under vacuum (10^{-3} bar) at 20 °C for 3 hours. Interestingly, no significant decrease was observed in the CO_2 uptake performance even after the 4th cycle of sorption–desorption. The CO_2 capture capacity was ~27 wt% after the 4th cycle. These data suggest that the IL $[N_{1,1,6,2OH}][4\text{-Triz}]$ can be regenerated in an energy efficient way rather than traditional nitrogen gas purging together with heating up to 80 °C (Fig. 4).

In order to gain deeper insights into the interactions of the CO_2 molecule with the IL, the $[N_{1,1,6,2OH}][4\text{-Triz}]$–$CO_2$ complex was characterized after CO_2 reaction using NMR and IR spectroscopic techniques. In the ^1H NMR spectrum of the IL $[N_{1,1,6,2OH}][4\text{-Triz}]$, an aromatic proton of the 1,2,4-triazolate anion [4-Triz] revealed a signal at 8.09 ppm before CO_2 absorption, which was shifted to 8.32 ppm after CO_2 absorption (see S5 in the ESI†). In the ^{13}C NMR spectrum, the signal for aromatic carbon at 153.54 ppm is shifted to 149.85 ppm along with a new signal of carbamate at 163.88 ppm after CO_2 absorption (see S11 in the ESI†). This major shift in the aromatic carbon of the 1,2,4-triazolate anion [4-Triz] is due to the lowering of aromaticity in the triazole ring after carbamate formation, which is further confirmed by DFT

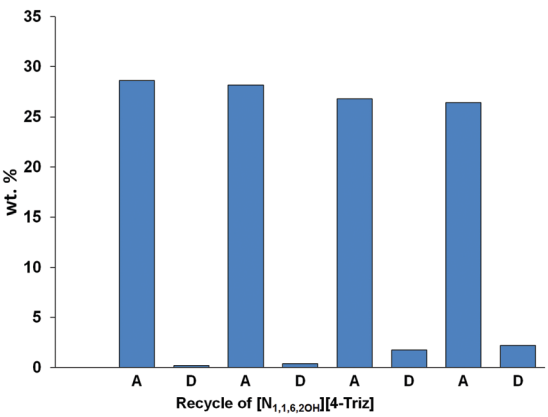

Fig. 4 Four cycles of the CO_2 absorption/desorption processes of the IL $[N_{1,1,6,2OH}][4\text{-Triz}]$. CO_2 absorption was performed out at 20 °C under 1 bar pressure and desorption was carried out at 20 °C under 10^{-3} bar pressure.

calculations. It could be noted that the CO_2 capture capacity of $[N_{1,1,6,2OH}][4\text{-Triz}]$ is 28.6 wt%, 1.57 mol of CO_2 per mol of IL under 1 bar pressure at room temperature (20 °C). However, theoretically the IL $[N_{1,1,6,2OH}][4\text{-Triz}]$ should capture 1 mol of CO_2 as it is a uni-negative ion although the 1,2,4-triazolate anion [4-Triz] have three nitrogen atoms.

From the DFT calculations (Fig. 6) it is observed that the N-4 nitrogen atom is the most negatively charged (−0.31) as compared with the other two nitrogen atoms (−0.24). Thus, carbamate formation is preferred at the N-4 position, which is further confirmed by NMR having one signal in the aromatic region. The IL $[N_{1,1,6,2OH}][4\text{-Triz}]$ showed ~1 equivalent CO_2 capture capacity at 40 °C suggesting a 1 : 1 reaction of the IL $[N_{1,1,6,2OH}][4\text{-Triz}]$ and a CO_2 molecule. This is because physical absorption of CO_2 has minor contribution to the CO_2 capture capacity at 40 °C due to the simultaneous adsorption–desorption process.

The ^{13}C solution NMR of the CO_2 saturated $[N_{1,1,6,2OH}][4\text{-Triz}]$ IL at 20 °C showed only one new signal for carbamate formation at 163.88 ppm. There is no information regarding the physically absorbed CO_2 or any other IL–CO_2 complex in the solution NMR spectrum of $[N_{1,1,6,2OH}][4\text{-Triz}]$ after CO_2 reaction. In order to obtain insights into the physically absorbed CO_2, we used isotopic grade $^{13}CO_2$ for our experiments. Initially, the IL $[N_{1,1,6,2OH}][4\text{-Triz}]$ was placed in a high pressure 5 mm Willmad NMR tube under a $^{13}CO_2$ atmosphere and allowed to react with the IL for several hours. Then, the $^{13}CO_2$ enriched IL sample was placed co-axially in 10 mm NMR with D_2O as an external lock for the ^{13}C NMR measurement. Interestingly, two new signals at 130.57 ppm and 158.67 ppm were observed in addition to the carbamate signal at 163.70 ppm. The new intense sharp signal at 130.57 ppm is due to the physically absorbed $^{13}CO_2$, whereas the signal at 158.67 ppm is probably due to the formation of carbonic acid (–OCO_2H) with the –OH group of the $[N_{1,1,6,2OH}]$ cation (see S12 in the ESI†).[23] Surprisingly, when the ^{13}C NMR measurement of the $^{13}CO_2$ enriched sample dissolved in D_2O was carried out, the signals at 130.57 ppm and 158.67 ppm disappeared again. However, after a large number of acquisitions, a small signal at 161.51 ppm was observed due to the formation of carbonate with the –OH group of the $[N_{1,1,6,2OH}]$ cation, which was further confirmed by the ^1H–^{13}C 2D heteronuclear multiple bond correlation (HMBC) experiment and found to be less stable in the solution form. The ^1H–^{13}C HMBC spectra are shown in the ESI† (S8) (Scheme 1).

To further confirm these findings, FTIR measurements were carried out to characterize the IL–CO_2 adducts. In the FTIR spectrum of the IL $[N_{1,1,6,2OH}][4\text{-Triz}]$ after CO_2 reaction, three additional stretching bands at 1677 cm^{-1}, 1635 cm^{-1} and a small band 2338 cm^{-1} were observed. The band at 1677 cm^{-1} is due to the formation of carbamate after CO_2 reaction. The band around 1635 cm^{-1} is attributed to the formation of carbonic acid, which disappeared by keeping the sample under vacuum (see S12 in the ESI†). The small band at 2338 cm^{-1} signified the presence of physically absorbed CO_2 in the IL $[N_{1,1,6,2OH}][4\text{-Triz}]$.[24]

^1H NMR diffusometry was carried out to investigate the self-diffusion of ions before and after CO_2 absorption. ^1H NMR signals of stimulated echo for all the studied ILs before and after absorbed CO_2 were observed in the whole temperature range from 20 °C to 90 °C, except for the IL $[N_{1,1,6,2OH}][Succ]$, for which the signal of the ^1H NMR stimulated echo was observed only at temperatures equal to and higher than 40 °C. This is due to the accelerated T_2 NMR relaxation of protons at lower temperatures (<40 °C) for this sample. Diffusion coefficients of anions and cations were calculated from the diffusion decays of the corresponding lines in the ^1H NMR spectra. All decays were well fitted in the equation of type eqn (1). Temperature dependences of D for the cations and anions before and after CO_2 adsorption are shown in Fig. 6.

A typical approach to the analysis of temperature dependence of D of ionic liquids is the Arrhenius type equation,[6] which described the temperature dependence of Ds in the form

$$D(T) = D_0 \exp\left(\frac{-E_D}{RT}\right) \quad (2)$$

where D_0 is a parameter that is independent of temperature, E_D is the molar activation energy of diffusion and R is the gas constant. However, this equation does not fit experimental dependences in many cases.[25] More universal forms of temperature dependences taking into consideration proximity of the system temperature to their glass transition temperature, T_0, is a Vogel–Fulcher–Tamman (VFT) VFT equation in the following form for diffusivity:[25]

$$D = D_0 \exp\left(\frac{-B}{(T - T_0)}\right) \quad (3)$$

where T_0 and B are adjustable parameters, $E_D = B{\cdot}R$. We have described $D(T)$ in Fig. 6 by fitting D_0, T_0 and B. B is a factor related to the activation energy and T_0 indicates a temperature at which free volume and mobility are reduced to zero.[43] The procedure of fitting was performed in two steps,

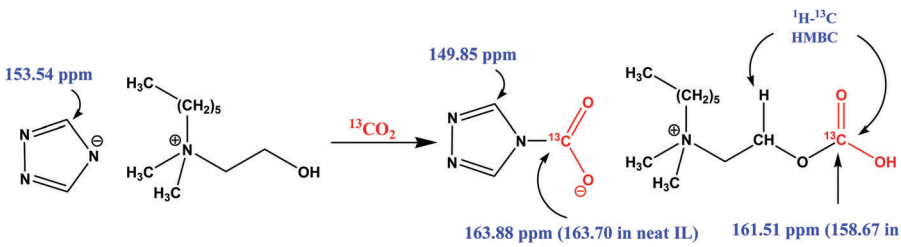

Scheme 1 The possible reaction of the CO_2 molecule with the cation and anion of the $[N_{1,1,6,2OH}][4\text{-Triz}]$ IL as revealed by ^{13}C NMR spectroscopy.

as described previously.[44] In the first step, ln(D) was plotted against $1/(T - T_0)$ and T_0 was selected to have a dependence linear. Uncertainty in this step was ±10 K. In the second step, the dependence was fitted by a linear regression to obtain the fitting parameters (D_0, B). Best results of the fitting are shown by solid (anions) and dotted (cations) lines in Fig. 5 and the corresponding fitting parameters as well as E_D are presented in Table 1. The temperature dependence of diffusivity for ions of all studied ILs fitted well into the VFT model over the whole studied temperature range.

From the ^{1}H diffusometry data, we observed some general features of self-diffusion of ions before and after CO_2 absorption in the studied ILs.

(1) There are two types of temperature dependences of diffusion coefficients for ILs before and after CO_2 absorption: firstly, the diffusion of cations and anions is equal for [$N_{1,1,6,2O4}$][Pyrz] (Fig. 5B) and [$N_{1,1,6,2OH}$][Succ] (Fig. 5E). Secondly the diffusion of anions is higher than the diffusion of cations for other three ILs (Fig. 5A–D). The first type reveals weak dissociation of ions while the second type suggests higher dissociation of ions. This difference in dissociation of ions is apparently related to the form of temperature dependence of Ds. In the first type, the Arrhenius type of temperature dependence (eqn (2)) is observed while in the second case VFT type (eqn (3)) is demonstrated. From Table 1, it is seen that for the first type of temperature dependence of ILs is characteristic of low T_0 and higher E_D as compared with

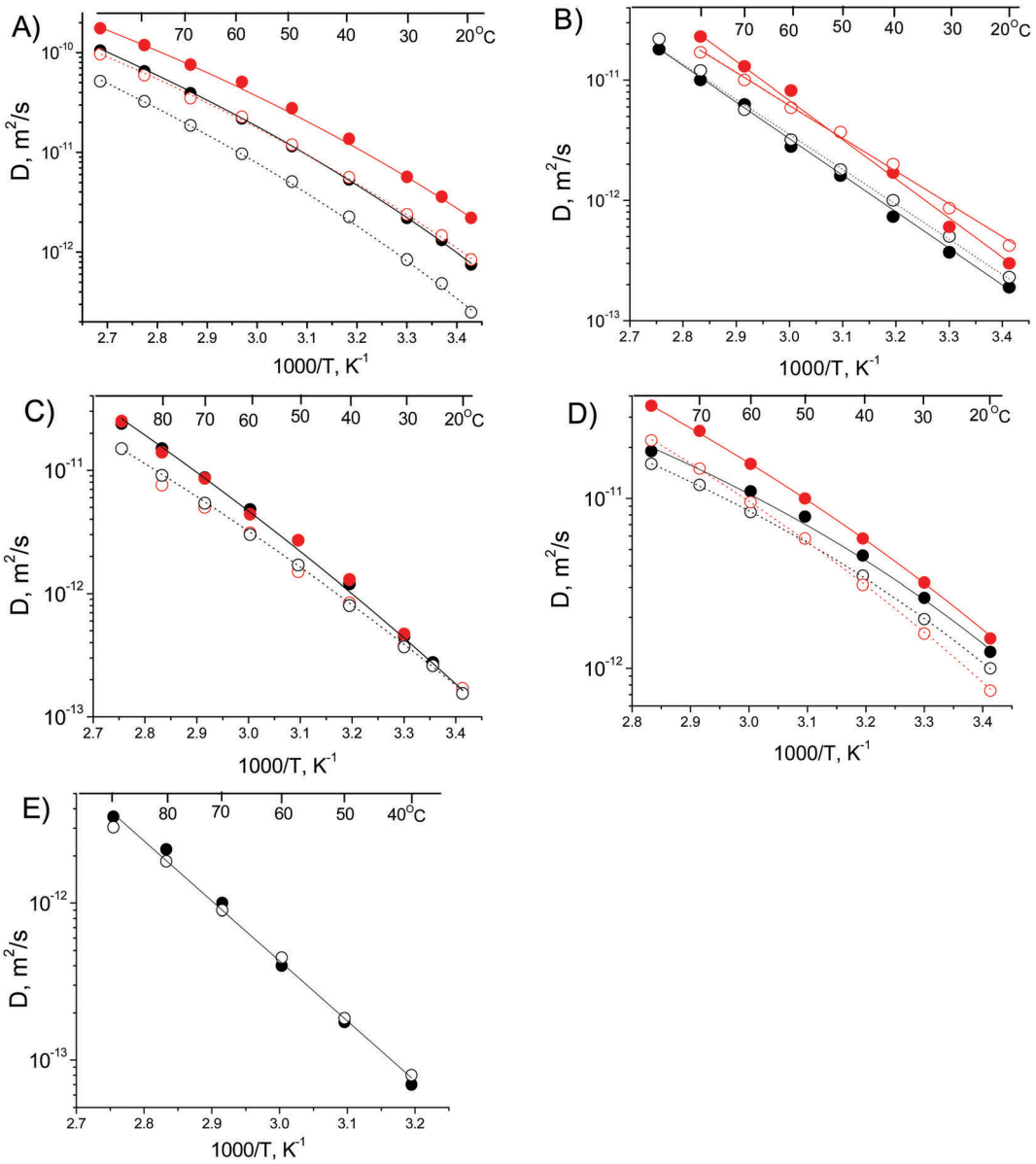

Fig. 5 Temperature dependences of diffusion coefficients obtained from ^{1}H PFG NMR DDs for: (A) [$N_{1,1,6,2OH}$][Imi],[13] (B) [$N_{1,1,6,2O4}$][Pyrz], (C) [$N_{1,1,6,2OH}$][4-Triz], (D) [$N_{1,1,6,2O4}$][4-Triz], (E) [$N_{1,1,6,2OH}$][Succ] before CO_2 capture (black) and after CO_2 capture (red). Solid symbols correspond to the anion and open symbols correspond to the cation. Lines correspond to the VFT equation fitting as shown in eqn (3) with the parameters of Table 1.

Table 1 VFT equation parameters and energies of activation for diffusion data of the studied ionic liquids. $[N_{1,1,6,2O4}][Pyrz]$ and $[N_{1,1,6,2OH}][Succ]$ obey the Arrhenius type temperature dependences

Ionic liquid	Ionic component	D_0, $m^2\ s^{-1}$	B	T_0, K	E_D, kJ mol^{-1} K^{-1}
$[N_{1,1,6,2OH}][Imi]$	Anion	1.9×10^{-7}	1510	170	12.6 ± 0.1
	Cation	1.6×10^{-7}	1620	170	13.5 ± 0.1
	Anion, after CO_2 absorption	1.35×10^{-7}	1340	170	11.1 ± 0.1
	Cation, after CO_2 absorption	1.2×10^{-7}	1440	170	12.0 ± 0.1
$[N_{1,1,6,2OH}][4\text{-Triz}]$	Anion, before and after CO_2 absorption	3.5×10^{-6}	2750	130	22.9 ± 0.1
	Cation, before and after CO_2 absorption	5.5×10^{-7}	2450	130	20.4 ± 0.1
$[N_{1,1,6,2O4}][4\text{-Triz}]$	Anion	1.4×10^{-9}	650	200	5.4 ± 0.1
	Cation	1.2×10^{-9}	660	200	5.5 ± 0.1
	Anion, after CO_2 absorption	2.1×10^{-8}	1170	170	9.7 ± 0.1
	Cation, after CO_2 absorption	2.3×10^{-8}	1270	170	10.6 ± 0.1
$[N_{1,1,6,2O4}][Pyrz]$	Anion	4.3×10^{-3}	7000	0	58.2 ± 0.1
	Cation	1.9×10^{-3}	6700	0	55.7 ± 0.1
	Anion, after CO_2 absorption	4.0×10^{-2}	7500	0	62.3 ± 0.1
	Cation, after CO_2 absorption	1.0×10^{-3}	6300	0	52.3 ± 0.1
$[N_{1,1,6,2OH}][Succ]$	Anion	1.25×10^{-1}	8800	0	73.2 ± 0.1
	Cation	1.25×10^{-1}	8800	0	73.2 ± 0.1

the second type of temperature dependence. Therefore, it takes higher T_0 and lower E_D for the dissociation of ions in the studied series of ILs. The higher viscosity of $[N_{1,1,6,2OH}][Succ]$ (ESI,† S10) can be related to the higher E_D for this IL.

(2) At high temperature (>60 °C) the diffusion coefficients of ions for different neat ILs increase in the order $[N_{1,1,6,2OH}][Succ] < [N_{1,1,6,2O4}][Pyrz] < [N_{1,1,6,2OH}][4\text{-Triz}] < [N_{1,1,6,2O4}][4\text{-Triz}] < [N_{1,1,6,2OH}][Imi]$, whereas at room temperature (20 °C) the order is $[N_{1,1,6,2OH}][Succ] < [N_{1,1,6,2O4}][Pyrz] < [N_{1,1,6,2OH}][4\text{-Triz}] < [N_{1,1,6,2OH}][Imi] < [N_{1,1,6,2O4}][4\text{-Triz}]$, which is the same as activation energies of diffusion E_D. $[N_{1,1,6,2OH}][Succ]$ and $[N_{1,1,6,2O4}][Pyrz]$ obey the Arrhenius type of temperature dependence with much higher E_Ds as compared with the others. Generally there is a certain relation between Ds and viscosities (ESI,† S10) in the whole series of these ILs.

(3) The diffusion coefficients of ions are increased after absorption of CO_2 which is demonstrated in a higher degree for $[N_{1,1,6,2OH}][Imi]$, $[N_{1,1,6,2O4}][4\text{-Triz}]$ and $[N_{1,1,6,2O4}][Pyrz]$. The absorption of CO_2 also leads to the increase in E_D for $[N_{1,1,6,2O4}][4\text{-Triz}]$ and for the anion in $[N_{1,1,6,2O4}][Pyrz]$, while it decreases only slightly in the case of $[N_{1,1,6,2OH}][Imi]$. Generally, the physisorption and chemisorption of CO_2 molecules are expected to increase the mass of the diffusion particle and thus decrease the diffusion coefficients of ions. However, the observed increase in the diffusion coefficients of ions in this case is most probably due to the decrease in the inter-ion interactions after CO_2 absorption in these ILs.

^{13}C NMR diffusometry was performed for the IL $[N_{1,1,6,2OH}][4\text{-Triz}]$ after absorbing ^{13}C enriched CO_2 gas in order to understand the diffusivity of both chemically reacted and physically absorbed CO_2 molecules. The ^{13}C NMR spectrum of the IL $[N_{1,1,6,2OH}][4\text{-Triz}]$ sample at 293 K demonstrated three intensive signals at 163 ppm, 158 ppm and 130 ppm as shown in figure S12 in the ESI.† Application of the NMR PFG technique leads to the diffusion decay of the signal amplitudes, from where diffusion coefficients were calculated using eqn (1). Signals at 163 and 158 ppm are characterized by diffusion coefficients typical for the cation and anion of $[N_{1,1,6,2OH}][4\text{-Triz}]$ ($\sim 1 \times 10^{-13}$ $m^2\ s^{-1}$), while the signal at 130 ppm showed the diffusion coefficient of $D = 1 \times 10^{-7}$ $m^2\ s^{-1}$. This demonstrates that the resonance line at 130 ppm belongs to the physically absorbed CO_2 gas in the IL $[N_{1,1,6,2OH}][4\text{-Triz}]$.[26]

The diffusion coefficient of the physically absorbed CO_2 gas is $\sim 10^6$ higher than the chemically bound one ($\sim 10^{-7}$ $m^2\ s^{-1}$ and $\sim 10^{-13}$ $m^2\ s^{-1}$, respectively at 293 K). It is known that the diffusion coefficient of CO_2 at normal pressure and temperature is $\sim 10^{-5}$ $m^2\ s^{-1}$.[27] Although the diffusion coefficient of CO_2 in the IL is less than that in the gas phase, however, the mobility of CO_2 is still very high compared to other components in the IL. The diffusivity of dissolved CO_2 in the IL is higher as compared with the CO_2 gas dissolved in water. The diffusivity of CO_2 dissolved in water is $\sim 10^{-9}$ $m^2\ s^{-1}$,[28] which is very close to the diffusion coefficient of water molecules. This is due to the strong network of hydrogen bonds formed in water, which incorporates CO_2 molecules and products of its dissociation. In contrast, the physically dissolved CO_2 does not interact that strongly with the IL. This is one of the plausible reasons that the dissolved CO_2 shows a relatively high translational mobility in the IL system.

In order to further support the experimental findings, we performed NICS (Nucleus-Independent Chemical Shifts) calculations using density functional theory (DFT) to evaluate the aromaticity behavior of the N-heterocyclic anions before and after CO_2 reaction. The NICS method is based on the negative of the magnetic shielding computed at the centre of the aromatic ring. A positive value implies antiaromaticity (paratropic ring current) and a negative value corresponds to aromaticity (diatropic ring current).[29–33] Conventionally, NICS values are at the geometrical center (GC) of the ring denoted as NICS(0) and 1 Å above/below the perpendicular plane of the

ring denoted as NICS(1). In this case due to the presence of symmetry in N-heterocyclic anions, both the ring critical point (RCP) and geometrical center (GC) coincide. According to the literature, NICS(1) (1 Å above/below the plane of the ring) is the best measure of the aromaticity descriptor than NICS(0) due to aromatic ring current and spurious contributions of the in-plane tensor components at the geometrical center of the ring. Further, the minimum effect of the local σ-bonding contributions is also observed at 1 Å above/below the molecular plane, thus, the out of plane tensor component of the NICS(1) values, $NICS_{zz}(1)$ shows an even better index of aromaticity.[34,35]

Current NICS calculations were computed through the gauge-including atomic orbital method (GIAO) implemented in GAUSSIAN 09[21,36] program using the B3LYP dft functional. Due to basis set dependencies of NICS values the aug-cc-pvtz basis set was used for all NICS calculations. Ghost atoms (symbol "Bq" from Gaussian 09 input) were used as the NICS probe without using basis functions and placed 1 Å above along the line perpendicular to the molecular plane and at the center of the molecular plane.

It is observed that the NICS(0) and NICS(1) values are less influenced after carbamate formation with N-heterocyclic anions in the ILs (Table 2). Whereas $NICS_{zz}(1)$ values increased significantly after carbamate formation as a result of CO_2 reaction with the N-heterocyclic anions of the ILs. The DFT data suggested a decrease in aromaticity of the anions after carbamate formation, which results in less pi–pi stacking interactions between the anions. The DFT optimized (gas phase) structures of 1,2,4-triazolate and the carbamate anion are shown in Fig. 6. The reduced pi–pi stacking interactions lead to faster diffusion of the anions and thus result in low viscosity of the ionic liquids upon CO_2 absorption.

Table 2 NICS values for aromatic N-heterocyclic anions and their carbamates calculated using density functional theory (in gas phase)

Name of the anion	NICS(0)	NICS(1)	$NICS_{ZZ}(1)$
4-Triazole	−11.63	−11.70	−36.89
4-Triazole carbamate	−11.35	−10.70	−31.69
Pyrazole	−12.29	−11.63	−36.70
Pyrazole carbamate	−12.21	−10.64	−31.33
Imidazole	−11.61	−10.74	−35.73
Imidazole carbamate	−11.18	−9.47	−29.27

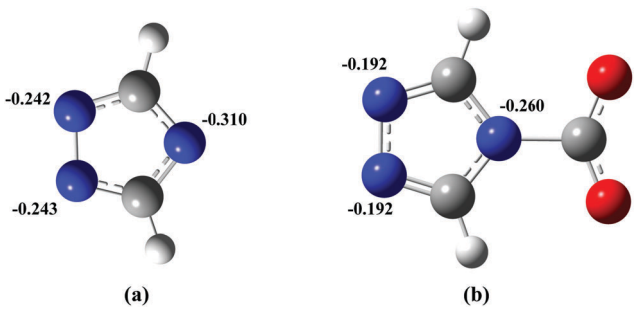

Fig. 6 DFT optimized (gas phase) structures of (a) 1,2,4-triazolate, and (b) carbamate anion with partial charge distribution after CO_2 reaction.

Conclusions

Ether functionalization of a choline based cation in the IL $[N_{1,1,6,2O4}][4\text{-Triz}]$ resulted in lowering of viscosity due to the elimination of hydrogen bonding as compared with a non-functionalized choline based IL $[N_{1,1,6,2OH}][4\text{-Triz}]$. However, CO_2 capture performance as well as thermal stability was decreased significantly by ether functionalization on the cation. The IL $[N_{1,1,6,2O4}][Pyrz]$ was found to be a semi-solid at room temperature and slow dissociation between cations and anions in the bulk system was observed from ^1H diffusion NMR data. The IL $[N_{1,1,6,2OH}][Imi]$ was less viscous and diffused faster as compared with the IL $[N_{1,1,6,2OH}][4\text{-Triz}]$ due to the presence of lesser number of hydrogen bond acceptor atoms. A significant dissociation between cations and anions was observed in both the ILs. The IL $[N_{1,1,6,2OH}][Succ]$ with non-aromatic N-heterocyclic anions was highly viscous and showed a lower CO_2 capture capacity compared to the ILs with aromatic N-heterocyclic anions. In addition, a very slow ionic mobility with low dissociation between cations and anions in the bulk system was observed. The IL $[N_{1,1,6,2OH}][4\text{-Triz}]$ showed the highest CO_2 capture capacity (28.6 wt%, 1.57 mol of CO_2 per mol of IL, 6.48 mol of CO_2 per kg of IL) at 20 °C and 1 bar pressure. in comparison with the previously reported N-heterocyclic (~8 wt%) ILs. The high CO_2 capture capacity of the IL $[N_{1,1,6,2OH}][4\text{-Triz}]$ is due to the contribution of the choline-based cation during the CO_2 capture process by the formation of carbonic acid (–OCO_2H) with the –OH group of the $[N_{1,1,6,2OH}]^+$ cation. The $[N_{1,1,6,2OH}][4\text{-Triz}]$–$CO_2$ adduct structure was confirmed by FTIR, ^{13}C NMR and ^1H–^{13}C HMBC NMR experiments utilizing ^{13}C labeled $^{13}CO_2$. The recyclability performance of $[N_{1,1,6,2OH}][4\text{-Triz}]$ showed that the IL can be recycled under vacuum at room temperature without using any nitrogen gas and heating. It is worth noting that the ionic mobility was increased significantly after CO_2 reaction in the case of ILs with aromatic N-heterocyclic anions, which can open a new area of research for low viscosity ionic liquids with promising CO_2 capture performance.

Conflicts of interest

The authors declare no conflicts of interest.

Acknowledgements

The Norrbotten Research Council (NoFo) and the Swedish Research Council are gratefully acknowledged for financially supporting this project.

References

1 N. V. Plechkova and K. R. Seddon, Applications of ionic liquids in the chemical industry, *Chem. Soc. Rev.*, 2008, **37**, 123–150.
2 J. W. Lee, J. Y. Shin, Y. S. Chun, H. B. Jang, C. E. Song and S.-G. Lee, Toward understanding the origin of positive

effects of ionic liquids on catalysis: formation of more reactive catalysts and stabilization of reactive intermediates and transition states in ionic liquids, *Acc. Chem. Res.*, 2010, **43**, 985–994.
3 T. Welton, Room-temperature ionic liquids: solvents for synthesis and catalysis, *Chem. Rev.*, 1999, **99**, 2071–2083.
4 H. Tokuda, K. Hayamizu, K. Ishii, Md. A. B. Hasan Susan and M. Watanabe, Physicochemical properties and structures of room temperature ionic liquids. 2. Variation of alkyl chain length in imidazolium cation, *J. Phys. Chem. B*, 2005, **109**, 6103–6110.
5 H. Tokuda, S. Tsuzuki, Md. A. B. Hasan Susan, K. Hayamizu and M. Watanabe, How ionic are room-temperature ionic liquids? An indicator of the physicochemical properties, *J. Phys. Chem. B*, 2006, **110**, 19593–19600.
6 P. Atkins and J. de Paula, *Atkin's Physical Chemistry*, Oxford University Press, 10th edn, 2014, p. 1008.
7 T. L. Greaves and C. J. Drummond, Protic ionic liquids: evolving structure–property relationships and expanding applications, *Chem. Rev.*, 2015, **115**, 11379–11448.
8 K. Damodaran, Recent NMR studies of ionic liquids, *Annu. Rep. NMR Spectrosc.*, 2016, **88**, 215–244.
9 R. Hayes, G. G. Warr and R. Atkin, Structure and nanostructure in ionic liquids, *Chem. Rev.*, 2015, **115**, 6357–6426.
10 A. E. Frise, T. Ichikawa, M. Yoshio, H. Ohno, S. V. Dvinskikh, T. Kato and I. N. Furo, Ion conductive behaviour in a confined nanostructure: NMR observation of self-diffusion in a liquid-crystalline bicontinuous cubic phase, *Chem. Commun.*, 2010, **46**, 728–730.
11 A. Filippov, F. U. Shah, M. Taher, S. Glavatskih and O. N. Antzutkin, NMR self-diffusion study of a phosphonium bis(mandelato)borate ionic liquid, *Phys. Chem. Chem. Phys.*, 2013, **15**, 9281–9287.
12 A. Filippov, M. Taher, F. U. Shah, S. Glavatskih and O. N. Antzutkin, Effect of length of long alkyl chains of cations on diffusion and density in pyrrolidinium bis(mandelato)borate ionic liquids, *Phys. Chem. Chem. Phys.*, 2014, **16**, 26798–26805.
13 S. Bhattacharyya, A. Filippov and F. U. Shah, Insight into the effect of CO_2 absorption on the ionic mobility of ionic liquids, *Phys. Chem. Chem. Phys.*, 2016, **18**, 28617–28652.
14 P. T. Callaghan, *Principles of Nuclear Magnetic Resonance Microscopy*, Clarendon, Oxford, 1991.
15 M. Ramdin, T. W. de Loos and T. J. H. Vlugt, State-of-the-art of CO_2 capture with ionic liquids, *Ind. Eng. Chem. Res.*, 2012, **51**, 8149–8177.
16 S. Bhattacharyya and F. U. Shah, Ether functionalized choline tethered amino acid ionic liquids for enhanced CO_2 capture, *ACS Sustainable Chem. Eng.*, 2016, **4**, 5441–5449.
17 M. Petkovic, J. L. Ferguson, H. Q. N. Gunaratne, R. Ferreira, M. C. Leitao, K. R. Seddon, L. P. N. Rebeloa and C. S. Pereira, Novel biocompatible cholinium-based ionic liquids: toxicity and biodegradability, *Green Chem.*, 2010, **12**, 643–649.
18 J. I. Santos, A. M. M. Goncalves, J. L. Pereira, B. F. H. T. Figueiredo, F. A. de Silva, J. A. P. Coutinho, S. P. M. Venturab and F. Goncalvesa, Environmental safety of cholinium-based ionic liquids: assessing structure–ecotoxicity relationships, *Green Chem.*, 2015, **17**, 4657–4668.
19 X.-D. Hou, Q.-P. Liu, T. J. Smith, N. Li and M.-H. Zong, Evaluation of Toxicity and Biodegradability of Cholinium Amino Acids Ionic Liquids, *PLoS One*, 2013, **8**, e59149.
20 J. E. Tanner, Use of the stimulated echo in NMR diffusion studies, *J. Chem. Phys.*, 1970, **52**, 2523–2526.
21 M. J. Frisch *et al.*, *Gaussian 09, Revision A. 01*, Gaussian, Inc., Wallingford, CT, 2009.
22 S. Seo, M. Q. Guzman, M. A. DeSilva, T. B. Lee, Y. Huang, B. F. Goodrich, W. F. Schneider and J. F. Brennecke, Chemically Tunable Ionic Liquids with Aprotic Heterocyclic Anion (AHA) for CO_2 Capture, *J. Phys. Chem. B*, 2014, **118**, 5740–5751.
23 C. Chatterjee and A. Sen, Sensitive colorimetric sensors for visual detection of carbon dioxide and sulfur dioxide, *J. Mater. Chem. A*, 2015, **3**, 5642–5647.
24 T. Seki, J.-D. Grunwaldt and A. Baiker, *In Situ* Attenuated Total Reflection Infrared Spectroscopy of Imidazolium-Based Room-Temperature Ionic Liquids under "Supercritical" CO_2, *J. Phys. Chem. B*, 2009, **113**, 114–122.
25 A. Noda, K. Hayamizu and M. Watanabe, Pulsed-gradient spin-echo ^1H and ^{19}F ionic diffusion coefficient, viscosity, and ionic conductivity of non-chloroaluminate room-temperature ionic liquids, *J. Phys. Chem. B*, 2001, **105**, 4603–4610.
26 H. Omi, T. Ueda, K. Miyakubo and T. Eguchi, Dynamics of CO_2 molecules confined in the micropores of solids as studied by ^{13}C NMR, *Appl. Surf. Sci.*, 2005, **252**, 660–667.
27 E. R. S. Winter, Diffusion properties of gases. Part IV. The self-diffusion coefficients of nitrogen, oxygen and carbon dioxide, *J. Chem. Soc.*, 1950, **1170**, 342–347.
28 R. E. Zeebe, On the molecular diffusion coefficients of dissolved CO_2, HCO_3^-, and CO_3^{2-} and their dependence on isotopic mass, *Geochim. Cosmochim. Acta*, 2011, **75**, 2483–2498.
29 P. Lazzereti, in *Prog. Nucl. Magn. Reson. Spectrosc.*, ed. J. W. Emsley, J. Feeney and L. H. Sutcliffe, Elsevier, Amsterdam, 2000, vol. 36, p. 1.
30 P. Lazzeretti, Assessment of aromaticity *via* molecular response properties, *Phys. Chem. Chem. Phys.*, 2004, **6**, 217–223.
31 J. Aihara, Nucleus-independent chemical shifts and local aromaticities in large polycyclic aromatic hydrocarbons, *Chem. Phys. Lett.*, 2002, **365**, 34–39.
32 N. H. Martin, D. M. Loveless, K. L. Main and D. C. Wade, Computation of through-space NMR shielding effects by small-ring aromatic and antiaromatic hydrocarbons, *J. Mol. Graphics Modell.*, 2006, **25**, 389–395.
33 P. v. R. Schleyer, C. Maerker, A. Dransfield, H. Jiao and N. J. R. van Eikema Hommes, Nucleus-Independent Chemical Shifts: A Simple and Efficient Aromaticity Probe, *J. Am. Chem. Soc.*, 1996, **118**, 6317–6318.
34 P. v. R. Scheleyer, M. Manoharan, Z. X. Wang, B. Kiran, H. J. Jiao, R. Puchta and N. J. R. v. E. Hommes, Dissected Nucleus-Independent Chemical Shift Analysis of π-Aromaticity and Antiaromaticity, *Org. Lett.*, 2001, **3**, 2465–2468.
35 C. Corminboeuf, T. Heine, G. Seifert, P. v. R. Schleyer and J. Weber, Induced magnetic fields in aromatic

[*n*]-annulenes—interpretation of NICS tensor components, *Phys. Chem. Chem. Phys.*, 2004, **6**, 273–276.

36 K. Wolinski, J. F. Hilton and P. Pulay, Efficient implementation of the gauge-independent atomic orbital method for NMR chemical shift calculations, *J. Am. Chem. Soc.*, 1990, **112**, 8251–8260.

37 A. Filippov, N. Azancheev, A. Gibaydullin, S. Bhattacharyya, O. N. Antzutkin and F. U. Shah, Dynamic properties of imidazolium orthoborate ionic liquids mixed with polyethylene glycol studied by NMR diffusometry and impedance spectroscopy, *Magn. Reson. Chem.*, 2017, DOI: 10.1002/mrc.4636.

38 C. Wang, X. Luo, H. Luo, D. Jiang, H. Li and S. Dai, Tuning the basicity of ionic liquids for equimolar CO_2 capture, *Angew. Chem., Int. Ed.*, 2011, **50**, 4918–4922.

39 S. Seo, M. Q. Guzman, M. A. DeSilva, T. B. Lee, Y. Huang, B. F. Goodrich, W. F. Schneider and J. F. Brennecke, Chemically tunable ionic liquids with aprotic heterocyclic anion (AHA) for CO_2 capture, *J. Phys. Chem. B*, 2014, **118**, 5740–5751.

40 X. Zhu, M. Song and Y. Xu, DBU-based protic ionic liquids for CO_2 capture, *ACS Sustainable Chem. Eng.*, 2017, **5**, 8192–8198.

41 C. Wang, H. Luo, D. Jiang, H. Li and S. Dai, Carbon dioxide capture by superbase-derived protic ionic liquids, *Angew. Chem., Int. Ed.*, 2010, **49**, 5978–5981.

42 R. Vijayraghavan, S. J. Pas, E. I. Izgorodina and D. R. MacFarlane, Diamino protic ionic liquids for CO_2 capture, *Phys. Chem. Chem. Phys.*, 2013, **15**, 19994–19999.

43 M. H. Cohen and D. Turnbull, Molecular transport in liquids and gases, *J. Chem. Phys.*, 1959, **31**, 1164–1169.

44 F. U. Shah, O. I. Gnezdilov and A. Filippov, Ion dynamics in halogen-free phosphonium bis(salicylato)borate ionic liquid electrolytes for lithium-ion batteries, *Phys. Chem. Chem. Phys.*, 2017, **19**, 16721–16730.